ACS OMEGA

Open Access

http://pubs.acs.org/journal/acsodf

Article

Adsorption Behavior of Different Components of a Polymer/Surfactant Composite Control System along an Injection-Production Channel in Sand Conglomerate Reservoirs

Yuanyuan Wang,* Dapeng Qin, and Shengdong Jiang

Cite This: *ACS Omega* 2024, 9, 40665−40675

Read Online

ACCESS | Metrics & More | Article Recommendations

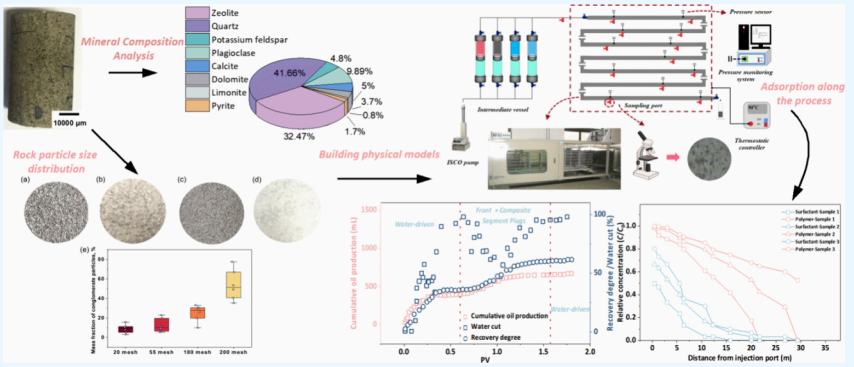

ABSTRACT: Sandy conglomerate reservoirs have become an important replacement area for unconventional energy to increase reserves and production. The polymer/surfactant composite control flooding system can effectively alleviate the water flooding front breakthrough caused by the interlayer or plane heterogeneity of the sand conglomerate reservoir and is an effective production method to reduce the water cutoff of the well and increase the oil recovery. In the process of controlling the oil displacement process of the system, the chromatographic separation effect was found due to the different viscosities of each component and the adsorption difference between the components and the rock, which weakened the development effect of the reservoir. It is necessary to study the adsorption law of each component of the complex controlled displacement system along the injection-production channel in the sand conglomerate reservoir. In this study, the microstructure and mineral composition of sandy conglomerates were determined by scanning electron microscopy and X-ray diffraction tests. The main particle size distribution was counted through a rock particle sieving experiment. A new characterization method called the large-size core physical model was used. The composite control system of sulfonate and betaine was used as the surfactant component, and the adsorption degree of each component in the displacement process was analyzed. The experimental results showed that the mass fraction of the sandy conglomerate increased with the decrease in particle size. The particles with a size of less than 0.08 mm account for a relatively high proportion, with a mass fraction of 60%. The content of brittle minerals, such as quartz and feldspar, in the glutenite was relatively high, and micrometer-sized pores and fractures were developed. The main factors affecting the viscosity of the composite system were the concentration and molecular weight of the polymer. The increase of injection volume of the flooding system is conducive to the maintenance of ultralow interfacial tension migration to the deep core. In the displacement process, when the polymer molecular chain was cut to a certain extent, the effect of throat shear was also slowed due to the short molecular chain. However, the shortened polymer molecules were more easily adsorbed on the surface of rock particles and the adsorption rate increased. The adsorption capacity of each component gradually decreased with the increase of the injection volume and injection concentration. The relative content of the composite control system and crude oil affects the type of emulsion, which undergoes a corresponding transformation during the driving process from a water-in-oil emulsion to an oil-in-water one. The research results of this paper enrich the mechanism of enhancing oil

continued...

Received: May 24, 2024
Revised: September 2, 2024
Accepted: September 10, 2024
Published: September 23, 2024

https://doi.org/10.1021/acsomega.4c04906
ACS Omega 2024, 9, 40665−40675

recovery of sand conglomerate reservoirs by polymer−surfactant composite regulation technology.

1. INTRODUCTION

Sand conglomerate reservoirs are important supplemented to global oil and gas production. For example, as the world's largest conglomerate oilfield so far, Xinjiang Mahu Oilfield has become an important substitute area for increasing unconventional energy storage and production.[1] For conglomerate reservoirs, water flooding is still an effective means to increase production and replenish formation energy.[2−4] As for conglomerate reservoirs, it has strong interlayer and stratification heterogeneity, which leads to premature water edge breakthrough at the end of oil wells, and the problems of high water cut and low sweep efficiency are particularly prominent.[5,6] Therefore, using tertiary oil recovery technology to develop conglomerates has become an effective production method.[7−9] In the enhanced oil recovery technology, composite flooding can greatly improve the utilization degree of reservoir crude oil.[10] The viscoelasticity of the polymer solution can effectively reduce the fingering phenomenon of the injected fluid in the reservoir and increase the swept volume of the injected fluid. Surfactants can greatly reduce the interfacial tension between crude oil and injected fluid, so as to achieve the purpose of stripping residual oil in pores.[11−13] Recent studies have found that as surfactants in sandstone mining, petroleum sulfonates can effectively improve the stripping efficiency of crude oil.[14] However, the effect of sulfonate surfactants is weakened in the higher-salinity reservoir environment. The reason for this situation is that due to the high electrolyte concentration, the adjacent micellar concentration of surfactant (CMC) is reduced, and the adsorbed active substance concentration of the interfacial monolayer is reduced, resulting in an increase in interfacial tension.[15] Betaine amphoteric surfactants have been widely used in oilfield exploitation due to their advantages because of low irritation, good hard water resistance, wide application range, and excellent biodegradability.[16] Moreover, betaine has the shear band behavior of wormlike micelles, which helps to improve oil displacement efficiency.[17] The interfacial properties of a single surfactant cannot achieve better results, and it needs to be used in combination with other types of surfactants to exert synergistic effects and better reduce the interfacial tension.[18] The compound system of betaine and anionic surfactant shows good interfacial activity and foaming performance and is also applicable in the reservoir environment with a certain salinity.[19] When the temperature reaches 60 °C, the compound system of sulfonate and betaine surfactant can provide better displacement efficiency in a high-salinity solution of 10.5%.[20] The interfacial tension of the compound system of sulfonate and amphoteric surfactant can be reduced to 10^{-2} mN/m at high salinity.[21] The adsorption capacity of amphoteric surfactants on sandstone is significantly higher than that of anionic surfactants, which can avoid the adsorption loss of sulfonates on rocks and improve the interaction effect with crude oil.[22]

In the process of compound flooding, due to the different polarities of each component in the oil displacement system, the separation of chemical agents will be caused. Different adsorption and desorption capabilities of chemical agents during reservoir migration lead to chromatographic separation of chemical agents, which seriously affects the development effect.[23] Laboratory experiments and field tests show that in the process of compound flooding, the breakthrough of polymer occurs before the breakthrough of surfactant. Surfactants have the largest adsorption capacity in the reservoir, followed by polymers.[24] Laboratory experiments are commonly used to characterize the adsorption of polymer/surfactant components during displacement. The effects of components on chromatographic separation, consumption, and loss of chemical agents in sandstone reservoirs can be understood through displacement experiments. The adsorption of each chemical component in the injection system in reservoir rocks has also been represented.[25−27] It shows that the adsorption of surfactants does not follow the Langmuir adsorption isotherm, but the adsorption of polymer chemicals does.[28] However, due to the size limitation of conventional displacement experiments, the chromatographic separation process between chemical agents is difficult to fully reflect. At present, there are few studies on the adsorption process along the injection-production channel of large sand conglomerate reservoirs. This work aims to elucidate the adsorption process of each dynamic component along the stream during the displacement process. To do this, the microporous structure and mineral composition of the sand conglomerate were examined by using scanning electron microscopy (SEM) and X-ray diffraction (XRD) techniques. The analysis focused on identifying the mineral species and their distribution patterns. Large-scale core physical simulation was applied to the experiment. The fluid samples at each position of the core were extracted, and the concentrations of each component and the pressures of each point were tested, respectively, to clarify the changes of each component and the utilization of crude oil. The emulsification effect during the displacement of crude oil by the composite control system was determined. The adsorption properties of the constituents of the polymer/surfactant composite control system were analyzed in terms of their displacement along the injection-production channel. The findings of this study can offer technical assistance for the efficient advancement of sand conglomerate reservoirs.

2. EXPERIMENTAL SECTION

2.1. Materials and Instruments. The polymer used in the experiments was an ultrahigh molecular weight polymer, which was provided by Wubei Oilfield. The surfactant was a mixture of 90% sodium dodecylbenzenesulfonate and 35% lauramidopropyl hydroxy sulfobetaine at a mass concentration of 1:1, which was produced by Qingdao USOLF Company, China. Crude oil and formation water used in the experiments were sampled from the field. The physical core model was used to simulate the reservoir conditions and was filled with granular sand into a tubular shape of 30 m with a diameter of 2.5 cm. The cationic surfactant Haiming 1622 was used as an indicator to test the surfactant concentration. The viscosity of crude oil was tested by a Brookfield DV-II+ viscometer, USA. Composite control system solution rheology was tested using a Brookfield DV-III ULTRA rheometer, USA. The interfacial tension between surfactant and crude oil was measured by a TX-500D rotary drop interfacial tension meter. XRD and SEM were used to measure the mineral composition and microstructure of the rock samples, respectively.

2.2. Particle Size Analysis of Sand Conglomerate. The cementation morphology of the core was dispersed by soaking and physical knocking to disperse it into core particles, and then

https://doi.org/10.1021/acsomega.4c04906
ACS Omega 2024, 9, 40665−40675

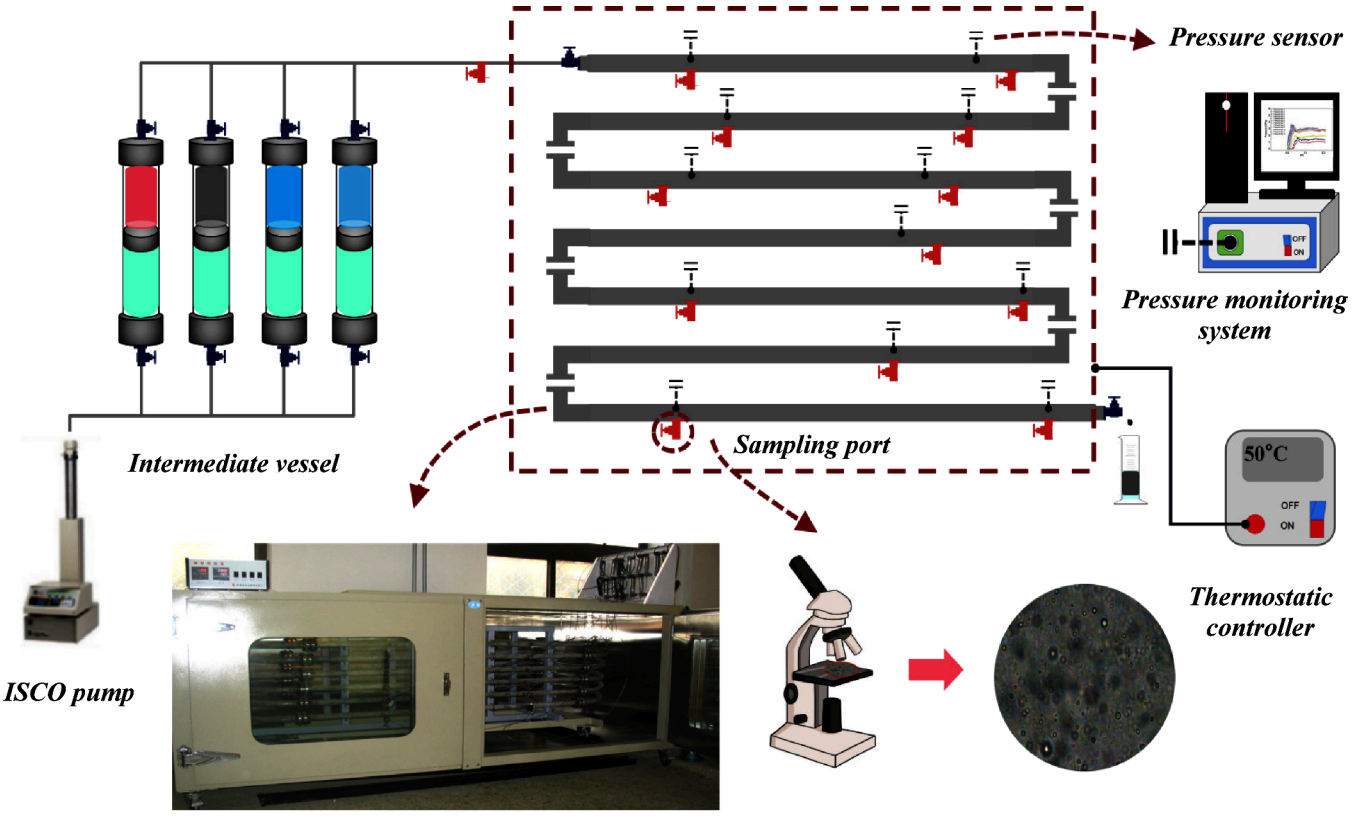

Figure 1. Displacement experimental flow of the polymer/surfactant complex regulatory system.

the core particles were filtered and classified through 20 mesh (0.8 mm), 55 mesh (0.3 mm), 180 mesh (0.09 mm), and 200 mesh (0.08 mm) sieves, respectively. The quality of sandstone with different particle sizes was calculated, and the proportion of particle size was obtained.

2.3. Analysis and Test Methods of a Polymer/Surfactant Composite Control System. The surfactants in the produced solution were measured by titration of anionic sulfonate using a microburet with a Haiming 1622 indicator. Since the formation water contained a variety of components and impurities, it interfered with the titration of sulfonates. Therefore, the two-component mixture with an average concentration (polymer concentration of 825 mg/L) was used as the background of the surfactant concentration test. The mass concentration of the polymer was determined by the contrast starch-cadmium iodide method through precipitation separation. The molecular weight of polyacrylamide in the polymer flooding production solution was determined by regression fitting through the comparison of the basic template data of the polymer original test by the viscosity difference method.

In the experiment of describing the dynamic chemical composition along the injection-production channel, the normalized concentration can be used to represent the relative content of each component:

$$C_n = \frac{C}{C_0} \tag{1}$$

where C_n is normalized concentration (dimensionless), mg/mL. C is the concentration of each component in the sample during the displacement of the complex control system, mg/mL. C_0 is the initial concentration of each component in the displacement sample, in mg/mL.

2.4. Characterization Method of Physical Parameters of a Polymer/Surfactant Composite Control System in the Core along the Injection-Production Channel. The physical simulation test process of the polymer/surfactant composite control system for ultralong sand-filled pipe is shown in Figure 1. There are 12 pressure measuring points in the injection and production channels, and the pressure changes in the whole displacement process are automatically monitored and recorded at an interval of 4 min. At the same time, 12 sampling points (sampling points and pressure points do not coincide) were set up to sample at different times of displacement. This dynamic simulation experiment device can explore the dynamic characteristics of oil displacement system migration in porous media, especially the transmission distance of pressure, which is an incomparable advantage of short-scale physical models with an end effect. The distribution of measuring pressure points and sampling points on the model tube is shown in Table 1.

The composite system was composed of 0.3% surfactant and 1200 mg/L ultrahigh molecular polymer. First, 0.0375 PV of 1200 mg/L ultrahigh molecular polymer solution was injected, then 1 PV of the composite solution was injected, and then the subsequent water flooding was carried out.

The specific experimental steps are as follows:

1. The core saturated with formation water was driven by crude oil until the formation water in the core is fully driven out. Core porosity, oil saturation, irreducible water saturation and other parameters were determined. The saturated crude oil core was aged for 24 h.
2. ISCO pump was turned on for the water flooding experiment, and water was injected at a constant speed of 0.03 mL/min until the water cut of the outlet reached

https://doi.org/10.1021/acsomega.4c04906
ACS Omega 2024, 9, 40665−40675

Table 1. Distribution of Pressure Measuring Points and Sampling Points

number	distance from the pressure measuring point to the entrance (m)	distance from the sampling point to the entrance (m)
1	0.44	0.44
2	1.28	1.46
3	2.99	2.99
4	5.54	5.54
5	7.22	6.38
6	9.65	10.64
7	11.44	12.28
8	15.74	15.74
9	20.01	20.01
10	21.68	21.68
11	26.81	26.81
12	28.34	29.36

98%, and then polymer flooding was carried out. The experimental temperature was 50 °C.

3. After polymer flooding, an intermediate container containing the composite system was opened. During the injection process, the sample was taken in time and the pressure was measured. The apparent viscosity, interfacial tension, adsorption capacity, and chromatographic separation of the solution at the outlet of each sampling point were recorded and tested. The emulsification phenomenon and the loss of composite system components were observed, and the degree of recovery was calculated.

3. RESULTS AND DISCUSSION

3.1. Analysis of Lithology and Particle Size Distribution of Sand Conglomerate. Partial core samples were extracted, and SEM was used to describe the microstructure and mineral morphology of the conglomerate. The SEM results of the three samples are listed in Figure 2. The clay mineral was the main cementing component, and the glutenite particles were presented in the form of contact cementation with intergranular pores. There were micron pores in the rock, the size of which was between 100 and 300 μm, mainly existing between the matrix. The microcracks were developed in the matrix, with a small scale and a scale of microns. There were complex components in the pores between the particles, and their morphology was like that of worms. In some rock samples, clay minerals are attached to the surface and natural microfractures, and the cementation is loose. In the scan map perpendicular to the bedding surface, the rock mineral particles are chaotic and uneven in size. Brittle minerals such as quartz, feldspar, dolomite, and clay crystal calcite develop easily to form cracks under the condition of reservoir ground stress, and the cracks are easily connected.

In order to clarify the distribution of particle size and mineral content in glutenite samples, the corresponding data were obtained by a sieving experiment and an XRD test. Figure 3 shows the main particle size distribution and mass fraction of the sand conglomerate. The mass fraction of conglomerates increases with the decrease in size. The particles with a size of less than 0.08 mm account for a relatively high proportion, with a mass fraction of 60%. The particle size mass fraction of 20 mesh (0.8 mm) is 8−20%.

The mineral composition of the conglomerate with different particle sizes was analyzed. The mineral composition of different particle sizes in one of the samples is shown in Figure 4. Quartz,

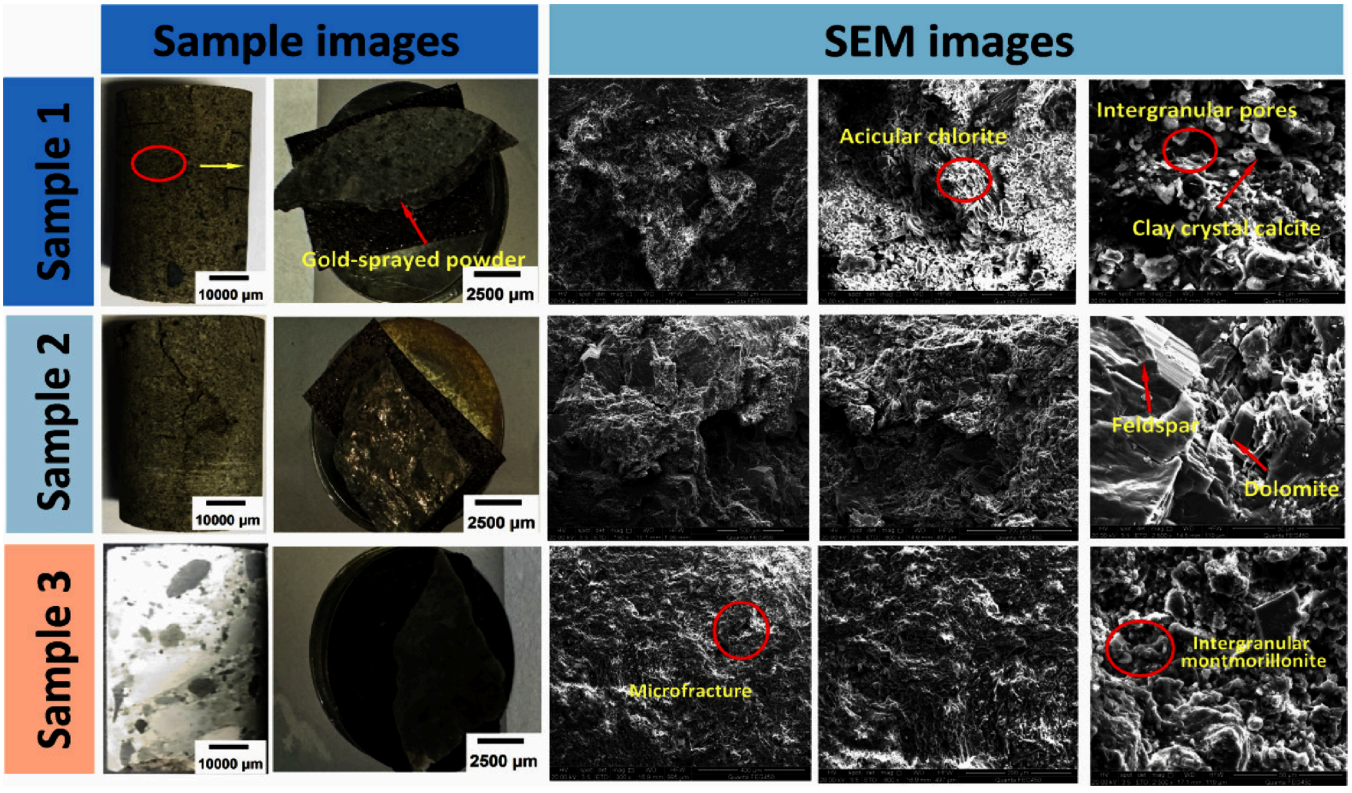

Figure 2. SEM test results of sandy conglomerate samples.

https://doi.org/10.1021/acsomega.4c04906
ACS Omega 2024, 9, 40665−40675

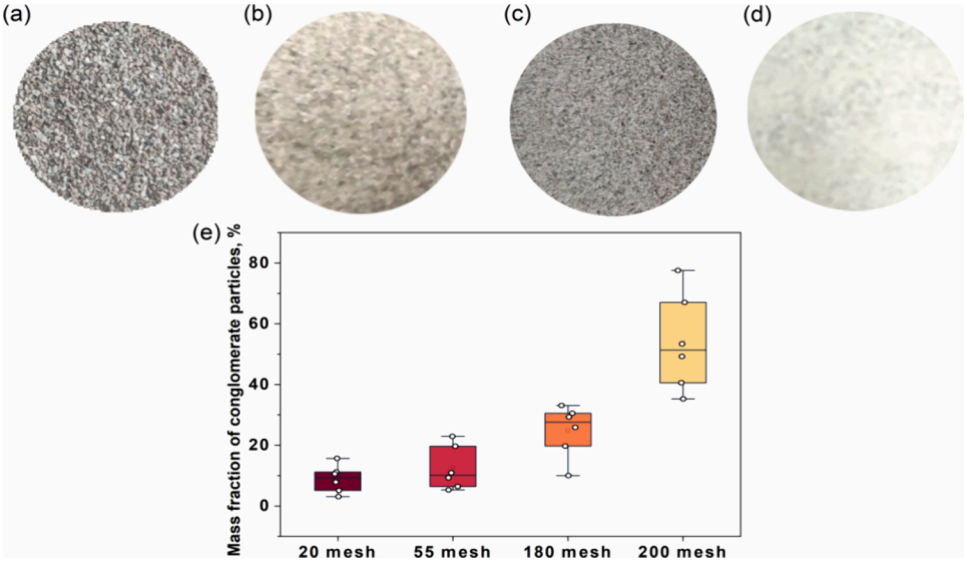

Figure 3. Sample and mass fraction of sand conglomerate filtered by a screen. The particle sizes of (a), (b), (c), and (d) are 20 mesh, 55 mesh, 180 mesh, and 200 mesh, respectively. (e) Proportion of particle size of conglomerate.

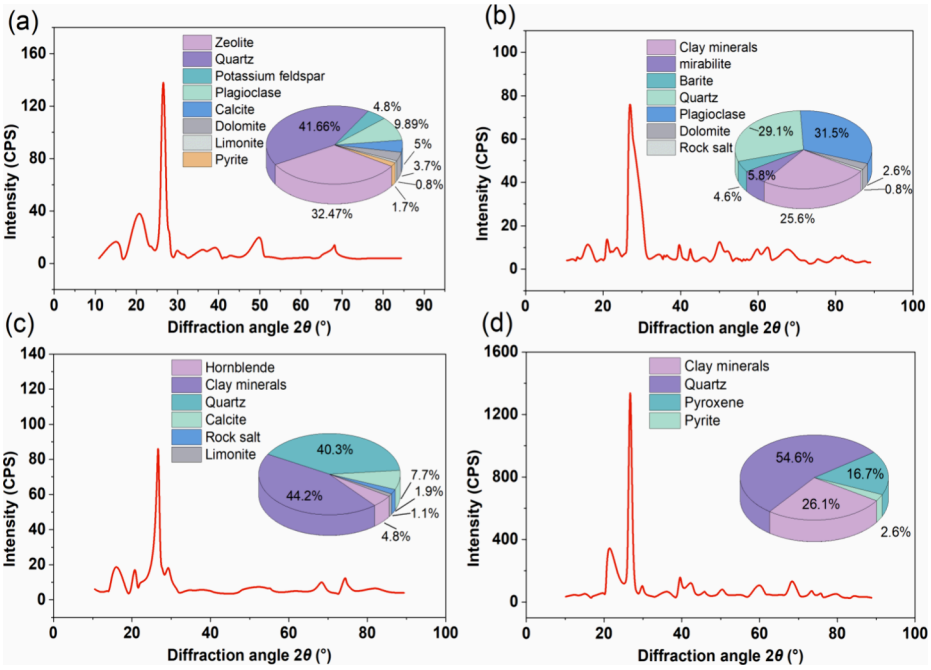

Figure 4. XRD test results of rock samples with different particle sizes. (a−d) Test results of minerals with particle sizes of 20, 55, 180, and 200 mesh, respectively.

feldspar, and clay minerals accounted for the main components, of which the quartz mass fraction accounted for 30−54%, feldspar 13−30% and clay minerals accounted for 25−44%. The test results were consistent with the SEM results.

3.2. Rheology Testing of a Composite Control System.

The thickening component of the composite control system is the polymer solution, the polymer solution is a non-Newtonian fluid, and the solution viscosity varies with the change of shear stress. The viscosity of the solution manifests itself as a phenomenon of diluted by shear. It is necessary to measure the rheology of the solutions used during the experiments. Figure 5 represents the rheological profiles and viscosity of the composite control system at temperatures of 50, 55, 60, 65, and 70 °C, with a polymer molecular weight of 19 million and a concentration of 1200 mg/L. The rheological profiles were fitted using the yield force-pseudoplastic fluid model (eq 2), and the results of the fitting are shown in Table 2:

$$\tau = \tau^{\circ} + kD^{n} \tag{2}$$

where τ is the shear stress, Pa. D is the shear rate, s^{-1}. k is the consistency factor, mPa s. n is the rheological index, dimensionless. τ° is the field force, Pa.

The tests utilize polymers with constant molecular weight and concentration. The temperature of the oil reservoir, which is influenced by its depth, is the only variable analyzed in this work, regarding the modification of the composite control system. The shear stress of the composite control system is directly proportional to the shear rate. The temperature and yield

https://doi.org/10.1021/acsomega.4c04906
ACS Omega 2024, 9, 40665−40675

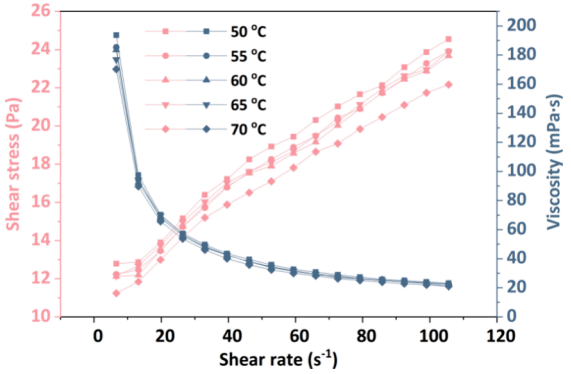

Figure 5. Rheological curves of the composite modulation system at different temperatures.

Table 2. Rheological Equations for Solutions of Composite Regulatory Systems

temperature (°C)	k (mPa s)	n	τ^o (N/m)	rheological equation
50	97.7	0.83	1.05	$\tau = 1.05 + 97.7D^{0.83}$ R^2 = 0.998
55	31.5	0.81	1.04	$\tau = 1.04 + 31.5D^{0.81}$ R^2 = 0.996
60	34.2	0.79	1.02	$\tau = 1.02 + 34.2D^{0.79}$ R^2 = 0.994
65	78.7	0.72	0.89	$\tau = 0.89 + 78.7D^{0.72}$ R^2 = 0.995
70	50.6	0.70	0.91	$\tau = 0.91 + 50.6D^{0.91}$ R^2 = 0.998

force have an impact on the solution, causing the rheological index of the fluid to decrease as the temperature rises. These findings suggest that the polymer solution in the system experiences more thinning under high temperatures and that the molecular structure is more prone to rupture. The viscosity change of the solution system shows a decreasing trend with the increase of shear rate, the shear rate decreases rapidly from 0 to 30 s^{-1}, and the viscosity decreases at a lower rate after further increase of shear rate. In addition, the solution viscosity is less affected by temperature compared to the shear rate, and the viscosity value needs to be further investigated to determine whether the crude oil in the core can be effectively driven under the current conditions.

3.3. Characterization of Nonpiston Displacement. When the initial interface between two mutually incompatible fluids, the driving phase and the driven phase, moves at a constant rate during the displacement process, instability of the leading edge of the displacement occurs when the fluid moves at a velocity greater than a certain critical velocity.[29] This phenomenon leads to a nonpiston flow at the leading edge of the expulsion and the formation of viscous fingers. The critical flow rate U_c for the unsteady phenomenon during the expulsion process can be expressed by eq 3:

$$\left(\frac{\mu_2}{k_2} - \frac{\mu_1}{k_1}\right)U_c + \left(\rho_2 - \rho_1\right)g\cos\theta = 0 \tag{3}$$

The viscous fingering phenomenon appears when the range of expulsion exceeds the maximum unstable wavelength (λ_m) of the spatial disturbance of the moving leading edge:

$$\lambda_m = \sqrt{3}\lambda_c \tag{4}$$

where the critical wavelength λ_c of the moving displacement front can be expressed by eq 5:

$$\lambda_c = 2\pi\left[\frac{\sigma}{\left(\frac{\mu_2}{k_2} - \frac{\mu_1}{k_1}\right)\left(U - U_c\right)}\right] \tag{5}$$

In these expressions, ρ, μ, and K, with subscripts 1 and 2 to distinguish the two liquids under consideration are density, viscosity, and effective permeability, respectively; g is the absolute value of gravitational acceleration; and cos θ is the directional cosine between the Cartesian coordinates and the effective permeability. u is the average volumetric velocity (volume of liquid injected per unit of total area perpendicular to the interface per unit of time). σ is the effective interfacial tension between the oil and water.

The maximum unsteady wavelength was calculated in conjunction with the current experimental conditions, and the data parameters are shown in Table 3.

Table 3. Experimental Displacement Parameters

μ_p (mPa s)	μ_o (mPa s)	K (10^{-3} μm^2)	ρ_w (g/cm^3)	ρ_o (g/cm^3)	σ (dyn/cm)
20	25	47.3	1.2	0.8	42

As the polymer solution is shear diluted, the viscosity at stabilization is taken into account in the computations. Combining the calculation formula yields the maximum unstable wavelength under the experimental circumstances. For fluid flow angles ranging from 0 to 90 deg, the maximum unstable wavelength (λ_m) is found to be between 2.84 and 3.0 cm. As the angle decreases, the maximum unstable wavelength value rises. Since the cross-sectional size of the lithology during the experiment is 2.5 cm, which is smaller than the unstable wavelength λ_m, the effect of viscous fingering on the experimental results can be neglected.

3.4. Analysis of Displacement Production Results. The change in production during the displacement process can directly reflect the displacement efficiency of the composite slug. The effect of composite solution displacement is evaluated through the experiment of ultralong core displacement. Table 4

Table 4. Physical Properties of Ultralong Sand-filled Pipe Cores

parameters	value
size of the model	L 30 m × φ 2.5 cm
absolute permeability	47.3 × 10^{-3} μm^2
porosity	12.1%
oil saturation	61%
volume of pores	1781 mL

shows the basic physical property parameters of the core. After water injection and compound solution injection, the change of production index in the whole process is shown in Figure 6.

It should be noted that injection PV refers to the ratio of injection volume to core pore volume, which represents the amount of liquid injected into the core. In the water flooding stage, the water injection volume was 0.61 PV, and the crude oil was 395.9 mL. At this time, the water cut was 98%. In the whole process, the water cut rose rapidly, and the accumulated oil production remained basically unchanged after 0.35 PV water

https://doi.org/10.1021/acsomega.4c04906
ACS Omega 2024, 9, 40665−40675

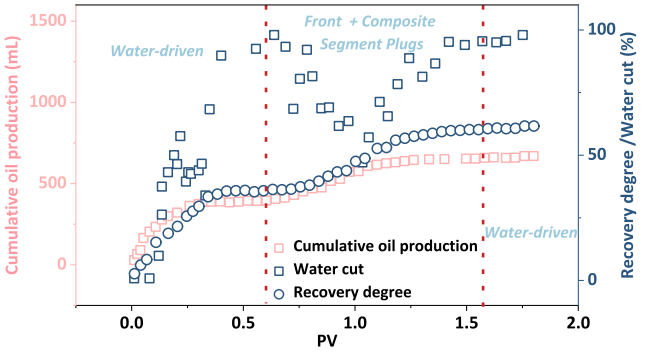

Figure 6. Evaluation of displacement effect of composite solution.

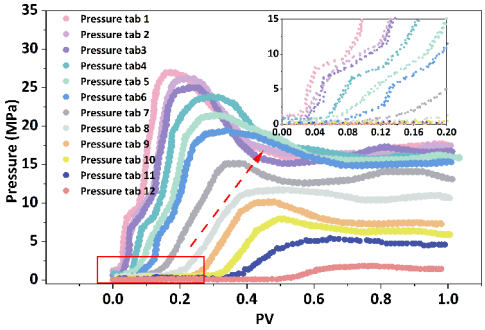

Figure 7. Pressure change curve in the process of compound displacement.

injection, which reached the limit of water flooding. The degree of water drive recovery was calculated, and the value was 36.4%. In order to ensure the effective function of the composite slug after water injection and not be diluted by the internal fluid of the core, a polymer preslug was required. The preslug was designed to be an ultrahigh polymer solution with a concentration of 1200 mg/L, and a protective fluid of 0.035PV was injected in the experiment. After the preslug was injected, 1 PV of the composite system was injected continuously. When the total amount of presolution and composite slug was 0.4 PV, the water cut decreased obviously, and the lowest dropped to 48%. At this time, cumulative oil production was on the rise. This was because the viscoelasticity of the polymer and the oil washing ability of the surfactant improved the oil displacement efficiency, which increased the swept volume of the displacement agent inside the core and used the residual crude oil under water flooding. With the continuous injection of the composite system, the water cut increased again, but the increase was slower than that due to water flooding. During the injection period, 260.9 mL of crude oil was produced, and the recovery degree increased by 24.0% on the basis of water flooding, and the oil increase effect was obvious. After the composite displacement, the water flooding was continued, the water cut reached 98% after water injection of 0.22 PV, and the experiment was stopped. The process produced 10 mL of crude oil, and the degree of recovery increased by 0.9%, which is close to the limit of recovery efficiency. Under the current experimental conditions, the total recovery of crude oil was 24% after injection of composite flooding fluid by 1 PV. The total recovery rate after composite flooding reached 61.7%, and the oil production effect was obvious. In order to clarify the migration state of the polymer and surfactant during the injection of the composite system into the core, samples were taken at different positions of the core. The interfacial tension, viscosity, surfactant, and polymer concentrations of the samples were tested.

The change of pressure during the displacement of the composite system directly reflects the difficulty of the injection in the field test. Figure 7 shows the dynamic pressure monitoring results during the injection of the composite system. In the process of injecting presolution by 0.035 PV, the pressure rose rapidly, and the closer the injection point was, the faster the pressure rose. After the composite system was continuously injected, the pressure increased further, reaching a maximum of 26.7 MPa at the first monitoring point. The farther the monitoring point was from the injection point, the lower the pressure peak. The peak pressure near the outlet dropped to 1.43 MPa, and the difference between the peaks was 0.53 PV. From the sampling observation, the crude oil production increased rapidly and the emulsification effect was obvious during this period of displacement. After the crude oil was displaced, the pressure dropped and remained stable. In the process of displacement, each pressure measuring point responded in sequence, and it can be inferred that the displacement front advances smoothly, which improves the swept volume, thus increasing the reservoir recovery rate.

The pressure dynamics of the subsequent water flooding stage is shown in Figure 8. Due to the large amount of liquid, the pump

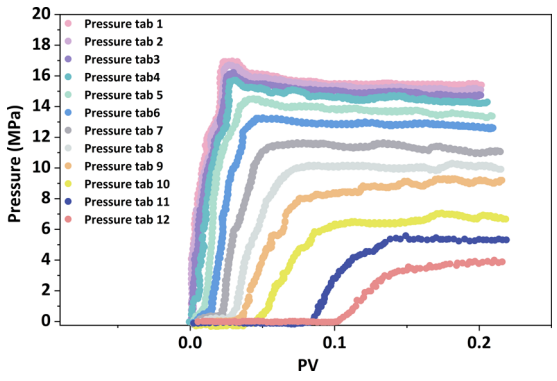

Figure 8. Pressure change curve in subsequent water flooding processes.

needs to be stopped during the water flooding process. After restarting the pump, the initial pressure of water flooding was reaccumulated and then tended to be stable. The pressure tended to be gentle after a short fluctuation. However, its stability value was relatively lower than the pressure value during the injection composite system, and the viscosity of the aqueous phase was the main determinant. The pressure dynamic in the water flooding stage showed that some emulsions continued to be pushed in the subsequent water flooding stage, but the pressure fluctuation was not obvious. The crude oil composition in this part of the liquid was low. After the injection, water was gradually diluted, a part of the oil was relodged in the pores, and a small part was produced with the liquid flow. The increase in recovery rate is small during water flooding.

In the subsequent water flooding stage, with the increase in the displacement distance, the variation range of injection pressure gradually decreased, indicating that there was a certain degree of particle migration in the local displacement process. In the subsequent water flooding stage, the equilibrium state established in the early stage was destroyed by water injection, especially the emulsion, and the high concentration of polymer

https://doi.org/10.1021/acsomega.4c04906
ACS Omega 2024, 9, 40665−40675

generated could lead to particle migration. As a result, the migration of these particles toward the outlet caused the distance between the pressure curves to widen.

3.5. Determination of Physical Parameters of a Polymer/Surfactant Composite Control System along the Injection-Production Channel in the Core. Samples at 12 different locations at different injection times were taken for analysis and testing. The polymer pore volume injected during sampling and the theoretical displacement front location are shown in Table 5.

Table 5. Time and Position Statistics of Composite System Samples

order of sampling	equivalent pore volume multiple of polymer injection (PV)	theoretical leading edge position of the converted polymer (m)
1	0.579	17.37
2	0.790	23.7
3	1	29.36

The sample viscosity and polymer concentration measured from different sampling points are listed in Figure 9. With the

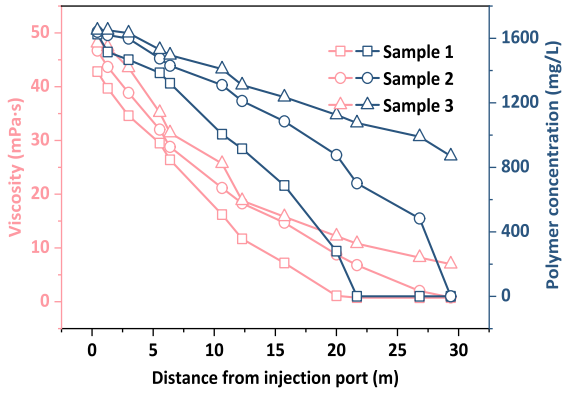

Figure 9. Changes of fluid viscosity at different sampling points.

increase in the injection amount of the composite system, the fluid viscosity at the same sampling position also increased accordingly. At the first sampling, the water cut at the production end was high and the fluid viscosity was low. With the increase in the flow distance of the composite system in the core, the viscosity of the corresponding sample also decreased. When the composite system was injected with 1 PV, the average decrease of viscosity at 0−15 m could reach 2.9 mPa s/m, and the decrease at 15−30 m was greatly slowed down to 0.84 mPa s/m. After the leading edge of the final composite system completely flowed in the core, the fluid viscosity at the outlet end was 7 mPa s, and the shear loss of viscosity was large. The polymer concentration corresponded to the change of viscosity, and the farther away from the injection point, the lower the concentration. With the increase in injection volume, the concentration of each sampling point also increased accordingly. Since the pore surface has fully absorbed the chemical agent injected in the early stage, the physical properties of the samples taken out in the later stage can be maintained at a certain level. The main factors affecting the viscosity of the composite system are the concentration and molecular weight of the polymer. In the process of displacement, the polymer was constantly adsorbed and degraded by chain breaking when it flowed in porous media, which led to the viscosity loss of the composite system. However, due to the adsorption of surfactants to rocks, which mitigated the adsorption loss of polymers, the polymer concentration decreased less than the viscosity. However, formation water is also a disadvantage to the viscosity of the polymer solution. Due to the high salinity of the formation water, the molecular chain of the polymer was compressed and could not be fully extended under the action of surface negative charge.

The polymer molecules in the crimping state can slow to a certain degree of shear. While for composite flooding, another important performance is the change of interfacial tension of the system (Figure 10). The interfacial tension of the fluid increased

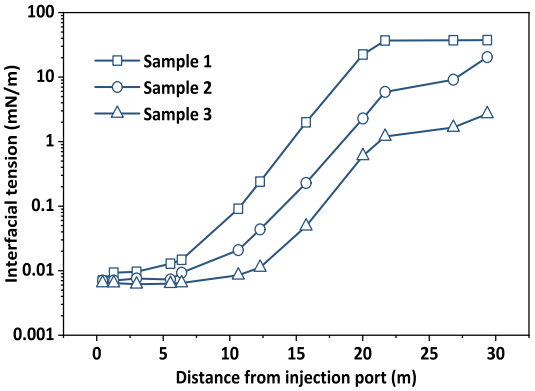

Figure 10. Changes of the interfacial tension at different sampling points.

rapidly with an increase in migration distance. The polymer molecules in the crimping state can slow down a certain degree of shear. During the initial sampling, although the theoretical leading edge of injection at this time was 17.37 m, the ultralow interfacial tension value (0−1.28 m) was reached only at the first and second sampling points. With the increase of migration distance, the interfacial tension was only maintained at about 10.64 m away from the entrance in the order of 10^{-2} mN/m. At 12.28−15.74 m, the interfacial tension reached 10^{-1}−10^{0}.

At the second sampling, the theoretical leading edge of the migration of the composite system reached 23.7 m, and the order of magnitude of 10^{-3} mN/m was extended to 6.38 m. At this time, 3.7 times PV of the composite system had been injected into the core near the inlet end. The orders of magnitude of 10^{-2} and 10^{-1} mN/m were 12.28 and 15.74 m, respectively. The injection front reached the outlet end, and the area of ultralow interfacial tension was about 1/3 of the core. By comparison, it was found that the increase in injection volume was conducive to the maintenance of ultralow interfacial tension in the deep migration of the core. When the composite system was injected with 1 PV, the actual ultralow interfacial tension was 35% of the theoretical migration distance, and the actual distance of the interfacial tension to maintain 10^{-2} mN/m was 52% of the theoretical migration distance. This situation could be explained by the adsorption of components in the rock and the chromatographic separation under the influence of the injection flow rate. It is necessary to focus on the change rule of the component concentration.

The change process of the molecular weight is similar to that of the concentration (Figure 11). When the migration distance was 10% of the total distance, the molecular weight loss was less than 5%. When the migration distance was 20% of the total

https://doi.org/10.1021/acsomega.4c04906
ACS Omega 2024, 9, 40665−40675

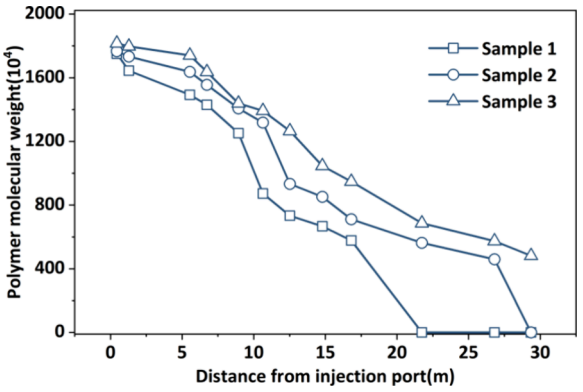

Figure 11. Changes of the polymer molecular weight at different sampling points.

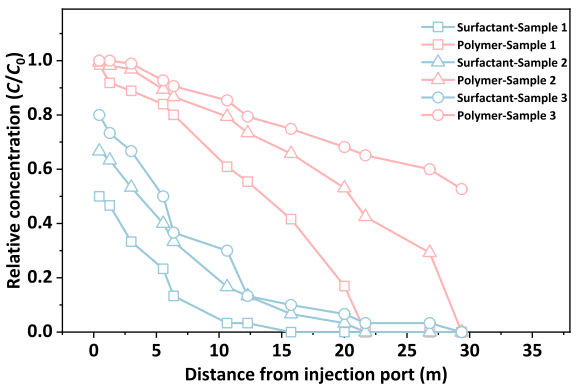

Figure 12. Concentration changes of composite system components along the injection-production channel.

distance, the molecular loss was about 20%. When the migration distance was 50% of the total distance, the molecular weight loss reached 45%. When the migration distance was 70% of the total distance, the molecular weight loss was more than 60%. When the injected polymer migrated to the outlet, the molecular weight loss rate reached more than 75% of the initial value. It could be found that the loss of molecular weight in the later period was rapid. The main reason was that this experiment started sampling after the injection reached 1 PV, so that the closer the front end was to the entrance end, the more polymer multiple was injected. Since there had been prior adsorption, the ability to "pull" the subsequent polymer molecular chain was reduced. Moreover, the polymer itself had a drag-reduction effect. Due to the influence of interface slip and other factors, it was equivalent to injecting 10 PV of polymer first and then sampling within the first 3 m distance. The molecular chain of the sample was protected to a certain extent, and the shear effect through the pore throat was not very large in the case of high permeability. Therefore, the molecular weight loss rate of the first segment was not large. In the later stages, the pore volume ratio of the injected polymer gradually decreased, and the "pulling" effect of adsorption on the rock surface gradually increased, resulting in rapid molecular chain fracture. Macroscopically, after a certain migration distance, such as 50% of the total distance, the molecular weight decreased rapidly and tended to be gentle soon. The reason for the gentle trend was that when the molecular chain was shortened to a certain extent, the effect of throat shear was also slowed down due to the short molecular chain when it migrated in porous media. For a pore throat of a certain size, sufficiently small molecules did not undergo shear degradation.

3.6. Chromatographic Separation Effect of Each Component in a Polymer/Surfactant Composite Control System. In the experiment, the concentrations of surfactant and polymer were, respectively, determined in the samples taken. The results of the sampling test are listed in Figure 12. The loss of surfactant was the most rapid, while the loss of polymer was relatively slow. The migration distance of the surfactant was much lower than the displacement front position. During the three sampling processes, the difference between the theoretical migration front and the actual detection position was 29.3, 15.6, and 8.7%, respectively. However, relatively speaking, the polymer migration distance was much larger. Generally, the component with the largest adsorption capacity was the surfactant; especially in the presence of high-salinity formation water, precipitation was also a factor that could not be ignored. When the polymer concentration was high, the surfactant concentration was at a low level. The concentration curve of the surfactant was concave down, while the front part of the polymer concentration curve was convex up. It can be seen that the adsorption rates of the three components on the core were quite different.

With the increase of the migration distance, the loss of surfactant increased rapidly. However, the loss rate was reduced by increasing the injection amount. It can be seen that the adsorption amount of surfactant decreased gradually with the increase in injection amount and injection concentration. The concentration of polymer changed in the same law, but the factors affecting the adsorption of polymer were different, such as the influence of inorganic ions, which led to a slight difference in their laws. In fact, adsorption is a dynamic equilibrium process. Under the condition that the saturated adsorption state was not reached, the absolute amount of adsorption increased with the increase in the external injection amount or concentration. When injected composite solution with 1 PV, the adsorption capacity of the polymer was almost similar and the polymer concentration was slightly higher in the early stage. This was due to the impenetrable pore volume of the polymer and the slow adsorption rate of the macromolecule; therefore, the initial concentration of polymer output was slightly higher. After a certain period of time, due to the mechanical shear of the polymer, the molecular chain was shortened, the adsorption rate was accelerated, and the inaccessible pore volume was reduced. The concentration of surfactant decreased rapidly from 0 to 20 m away from the injection point, the loss rate of surfactant concentration was close to 97%, and the action distance was relatively limited. Most researchers assume that the lower the injection velocity, the greater the adsorption capability of rock minerals to polymers and surfactants, resulting in stability. This is because the contact period between the solution and the rock core is greater at low injection velocity, resulting in increased adsorption. The influence of injection velocity on rock adsorption capacity is not discussed further in this article.[30,31]

3.7. Emulsification Effect Evaluation of a Polymer/Surfactant Composite Control System. In the process of displacement, due to chromatographic separation, the adsorption position of the surfactant was far away from the displacement front. The emulsification phenomenon in the sample was found near the inlet end. The microscopic morphology of the samples with obvious emulsification is shown in Figure 13. With the increase of the total injection amount of the system, the sampling points that produced

https://doi.org/10.1021/acsomega.4c04906
ACS Omega 2024, 9, 40665−40675

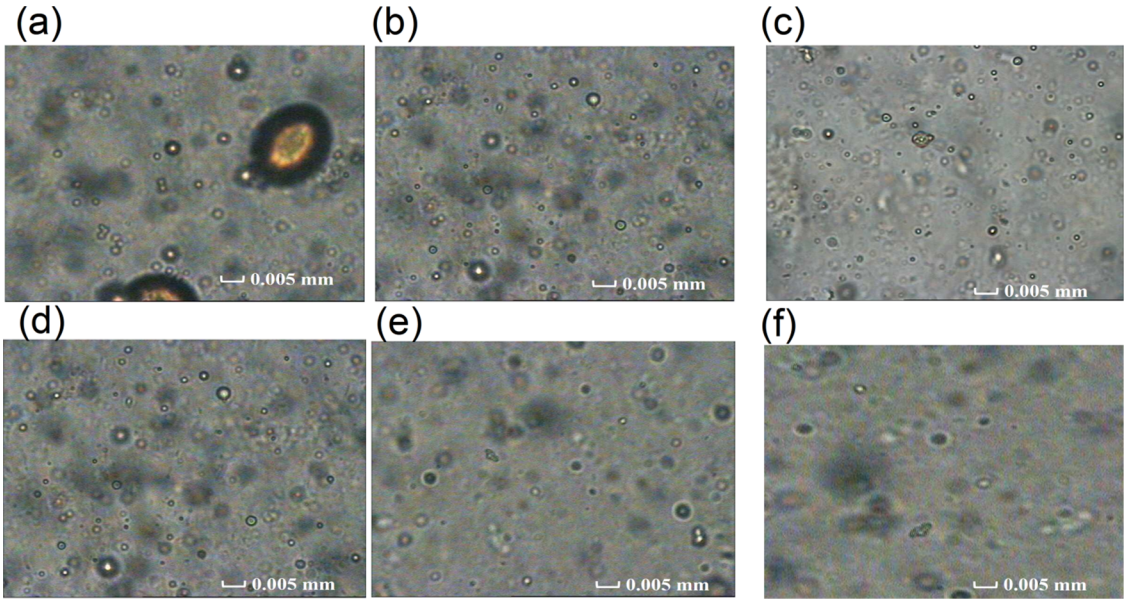

Figure 13. Emulsification effect of the composite system in the displacement process (400 times magnification). (a,d) First sampling at sampling points 4 and 5 (5.54−6.38 m from the injection port). (b,e) Second sampling at sampling points 6 and 7 (10.64−12.28 m from the injection port). (c,f) Third sample at sampling points 8 and 9 (15.74−20.01 m from the injection port).

emulsification obviously moved toward the displacement front. With the continuous migration of emulsions, the particle density and viscosity of emulsions were decreasing, and the type of emulsions was also changing.[32] At the initial stage, the emulsion was mainly a water-in-oil emulsion (Figure 13a−d). The proportion of oil and water in the middle stage was similar. At the third sampling, the emulsion was mainly oil-in-water emulsion. This result could be explained by the fact that the residual oil in the porous media gradually decreased with the increase of the injection volume. Especially at the third sampling, the residual oil saturation was low, about 28.7%, the amount of available oil was reduced, and the number of emulsion droplets was reduced. The type of emulsion was affected by the relative content of oil and water, and the corresponding transformation occurred.

4. CONCLUSIONS

Based on the micropore structure, particle size distribution, and mineral composition of the conglomerate reservoir, the adsorption of each component in the emulsion control system of polymer/sulfonate and betaine along the injection-production channel was analyzed. The results showed that the composite flooding could effectively alleviate the breakthrough of the water flooding front caused by the heterogeneity of the sandy conglomerate reservoir, which was an effective production method to improve the recovery rate. The proportion of sandy conglomerate particle size in the samples increased with a decrease of size. The main factors affecting the viscosity of the composite system were the concentration and molecular weight of the polymer. The increase of the injection volume of the oil displacement system was beneficial to the maintenance of the ultralow interfacial tension in the deep migration of the core, so as to improve the utilization of the residual oil in the reservoir. In the process of displacement, after the polymer molecular chain was sheared, the polymer molecules were more easily adsorbed on the surface of the rock particles and the adsorption rate increased. The polymer displacement toward the outlet was characterized by a reduction in molecular weight exceeding 75% of its original value. As the distance from the entry decreased, a greater number of polymer multiples were injected, resulting in a decreased capacity to break the molecular chain of the following polymers. The surfactant exhibits a concentration loss rate of around 97% throughout the displacement process and demonstrates a significant adsorption capability in the conglomerate reservoir. The adsorption capacity of each component gradually decreased with the increase of injection volume and injection concentration. The type of emulsion produced was transformed from a water-in-oil emulsion to an oil-in-water emulsion by the influence of the displacement agent and the relative content of oil. This study is of great significance for the effective utilization of a sand conglomerate reservoir and provides technical support for the application of polymer/surfactant enhanced oil recovery.

AUTHOR INFORMATION

Corresponding Author

Yuanyuan Wang − *Key Laboratory of Enhanced Oil & Gas Recovery of Ministry of Education, Northeast Petroleum University, Daqing 163318, P. R. China;* orcid.org/0009-0008-7655-6335; Email: yyw_petrol@163.com

Authors

Dapeng Qin − *No.6 Oil Production Plant, PetroChina Changqing Oilfield Company, Xi'an 710018, China*

Shengdong Jiang − *College of Chemistry Chemical Engineering, Daqing Normal University, Daqing 163111, China*

Complete contact information is available at: https://pubs.acs.org/10.1021/acsomega.4c04906

Author Contributions

Y.W.: conceptualization, methodology, data curation and analysis, writing—original draft. D.Q.: investigation, resources. S.J.: supervision, writing—review and editing.

Notes

The authors declare no competing financial interest.

https://doi.org/10.1021/acsomega.4c04906
ACS Omega 2024, 9, 40665−40675

■ ACKNOWLEDGMENTS

This research was funded by the National Natural Science Foundation of China (Key fundamental issues of discontinuous variable circulation of active nanofluids for enhanced recovery in offshore high-temperature and high-salinity oilfields, No. U22B6005).

■ REFERENCES

(1) Hou, Q.; Zhu, Y.; Luo, Y.; Weng, R.; Guoqing, J. Studies on nitrogen foam flooding for conglomerate reservoir. In *SPE EOR Conference at Oil and Gas West Asia*; SPE: 2012; p SPE-152010.
(2) Tan, F.; Li, H.; Xu, C.; Li, Q.; Peng, S. Quantitative evaluation methods for water-flooded layers of conglomerate reservoir based on well logging data. *Pet. Sci.* **2010**, *7*, 485−493.
(3) Gao, P. K.; Li, G. Q.; Tian, H. M.; Wang, Y. S.; Sun, H. W.; Ma, T. Differences in microbial community composition between injection and production water samples of water flooding petroleum reservoirs. *Biogeosciences* **2015**, *12* (11), 3403−3414.
(4) Yin, S.; Chen, Y.; Wu, X. Different pore structure modalities in sandy conglomerate reservoirs and their forming mechanisms. *Arab. J. Geosci.* **2018**, *11* (21), 654.
(5) Li, Y.; Tan, J.; Mou, S.; Liu, C.; Yang, D. Experimental study on waterflooding development of low-amplitude reservoir with big bottom water. *J. Pet. Explor. Prod. Technol.* **2021**, *11* (11), 4131−4146.
(6) Cheng, H.; Yuan, F.; Zhang, S.; Li, L.; Luo, X.; Chen, B. Investigation on Water Invasion Mode and Remaining Oil Utilization Rules of Fractured-Vuggy Reservoirs: A Case Study of the Intersection Region of S99 Unit in Tahe Oilfield. *Processes* **2023**, *11* (6), 1833.
(7) Liu, Z.; Li, Y.; Chen, X.; Chen, Y.; Lyu, J.; Sui, M. The optimal initiation timing of surfactant-polymer flooding in a waterflooded conglomerate reservoir. *SPE J.* **2021**, *26* (04), 2189−2202.
(8) Liu, Z.; Li, Y.; Leng, R.; Liu, Z.; Chen, X.; Hejazi, H. Effects of pore structure on surfactant/polymer flooding-based enhanced oil recovery in conglomerate reservoirs. *Pet. Explor. Dev.* **2020**, *47* (1), 134−145.
(9) Liu, Z.; Li, Y.; Lv, J.; Li, B.; Chen, Y. Optimization of polymer flooding design in conglomerate reservoirs. *J. Pet. Sci. Eng.* **2017**, *152*, 267−274.
(10) Hillary, A.; Taiwo, O. A.; Mamudu, A.; Olafuyi, O. Analysis of ASP Flooding in a Shallow Oil Reservoir in the Niger Delta. In *SPE Nigeria Annual International Conference and Exhibition*; 2016.
(11) Olajire, A. A. Review of ASP EOR (alkaline surfactant polymer enhanced oil recovery) technology in the petroleum industry: Prospects and challenges. *Energy* **2014**, *77*, 963−982.
(12) Sharma, H.; Dufour, S.; Arachchilage, G. W. P.; Weerasooriya, U.; Pope, G. A.; Mohanty, K. Alternative alkalis for ASP flooding in anhydrite containing oil reservoirs. *Fuel* **2015**, *140*, 407−420.
(13) Bera, A.; Mandal, A.; Guha, B. B. Synergistic effect of surfactant and salt mixture on interfacial tension reduction between crude oil and water in enhanced oil recovery. *J. Chem. Eng. Data* **2014**, *59* (1), 89−96.
(14) Pachón Contreras, Z. D. P.; Rojas Ruíz, F. A.; Rondón Antón, M. J.; Vidal-Prada, J. C.; Pulido-Solano, F. A. Petroleum sulfonates preparation and evaluation for chemical enhanced oil recovery in Colombian oil fields. *Cienc. Tecnol. Futuro* **2014**, *5* (5), 55−73.
(15) Wang, Z.; Li, P.; Ma, K.; Chen, Y.; Penfold, J.; Thomas, R. K.; Venero, D. A. The structure of alkyl ester sulfonate surfactant micelles: The impact of different valence electrolytes and surfactant structure on micelle growth. *J. Colloid Interface Sci.* **2019**, *557*, 124−134.
(16) Yang, H.; Zhang, H.; Zheng, W.; Zhou, B.; Zhao, H.; Li, X.; Galkin, S. V. Effect of hydrophobic group content on the properties of betaine-type binary amphiphilic polymer. *J. Mol. Liq.* **2020**, *311*, No. 113358.
(17) Kelleppan, V. T.; King, J. P.; Butler, C. S.; Williams, A. P.; Tuck, K. L.; Tabor, R. F. Heads or tails? The synthesis, self-assembly, properties and uses of betaine and betaine-like surfactants. *Adv. Colloid Interface Sci.* **2021**, *297*, No. 102528.
(18) Zhong, H.; Yang, T.; Yin, H.; Lu, J.; Zhang, K.; Fu, C. Role of alkali type in chemical loss and ASP-flooding enhanced oil recovery in sandstone formations. *SPE Reservoir Eval. Eng.* **2020**, *23* (02), 431−445.
(19) Wang, R.; Li, Y.; Li, Y. Interaction between cationic and anionic surfactants: detergency and foaming properties of mixed systems. *J. Surfactants Deterg.* **2014**, *17*, 881−888.
(20) Liu, X.; Chen, Z.; Cui, Z. Fatty alcohol polyoxyethylene ether sulfonate for foam flooding in high-salinity and high-temperature reservoir conditions. *Colloids Surf., A* **2021**, *629*, No. 127366.
(21) Xiao, Z.; Dexin, L.; Yue, L.; Lulu, L.; Jie, Y. Synergistic effects between anionic and amphoteric surfactants on promoting spontaneous imbibition in ultra-low permeability reservoirs: study of mechanism and formula construction. *Colloids Surf., A* **2021**, *625*, No. 126930.
(22) Mannhardt, K.; Schramm, L. L.; Novosad, J. J. Adsorption of anionic and amphoteric foam-forming surfactants on different rock types. *Colloids Surf.* **1992**, *68* (1−2), 37−53.
(23) Guo, H.; Li, Y.; Wang, F.; Gu, Y. Comparison of strong-alkali and weak-alkali ASP-flooding field tests in Daqing oil field. *SPE Prod. Oper.* **2018**, *33* (02), 353−362.
(24) Farajzadeh, R.; Matsuura, T.; van Batenburg, D.; Dijk, H. Detailed modeling of the alkali/surfactant/polymer (ASP) process by coupling a multipurpose reservoir simulator to the chemistry package PHREEQC. *SPE Reservoir Eval. Eng.* **2012**, *15* (04), 423−435.
(25) Demin, W.; Jiecheng, C.; Junzheng, W.; Zhenyu, Y.; Yuming, Y.; Hongfu, L.Summary of ASP pilots in Daqing oil field. In *SPE International Improved Oil Recovery Conference in Asia Pacific*; SPE: 1999; p SPE-57288.
(26) Wang, J.; Yuan, S.; Shi, F.; Jia, X. Experimental study of chemical concentration variation of ASP flooding. *Sci. China, Ser. E: Technol. Sci.* **2009**, *52* (7), 1882−1890.
(27) Shen, G.; Zhang, F.; Yang, B.; Chu, C.; Liang, X. A novel amide stationary phase for hydrophilic interaction liquid chromatography and ion chromatography. *Talanta* **2013**, *115*, 129−132.
(28) Li, D.; Shi, M.; Wang, D.; Li, Z. Chromatographic separation of chemicals in alkaline surfactant polymer flooding in reservoir rocks in the daqing oilfield. In *SPE International Conference on Oilfield Chemistry*; SPE: 2009; p SPE-121598.
(29) Chuoke, R. L.; Van Meurs, P.; van der Poel, C. The instability of slow, immiscible, viscous liquid-liquid displacements in permeable media. *Trans. AIME* **1959**, *216* (01), 188−194.
(30) Sazali, R. A.; Roslan, M. S.; Jarrahian, K. Adsorption study of acrylamide-tertiary-butyl sulfonate (ATBS)/acrylamide copolymer in polymer flooding enhanced oil recovery (EOR) process. In *Journal of Physics: Conference Series*; IOP Publishing: 2019; Vol. *1349*, No. 1, p 012125.
(31) Borovina, A.; Reina, R. E. H.; Clemens, T.; Hoffmann, E.; Wegner, J.; Steindl, J. Polymer Selection for Sandstone Reservoirs Using Heterogeneous Micromodels, Field Flow Fractionation and Corefloods. In *SPE Improved Oil Recovery Conference*; SPE: 2022; p D011S009R003.
(32) Zhang, J.; Yuan, H.; Zhao, J.; Mei, N. Viscosity estimation and component identification for an oil-water emulsion with the inversion method. *Appl. Therm. Eng.* **2017**, *111*, 759−767.

https://doi.org/10.1021/acsomega.4c04906
ACS Omega 2024, 9, 40665−40675